Correlation between input and output parameters of microbial fuel cell

Ganesan V. Murugesu[1], Saiful Nizam Khalid[1], Hussain Shareef[2], Saad Saleem Khan[2]
[1]Department of Electrical Power Engineering, Faculty of Electrical Engineering, Universiti Teknologi Malaysia, Johor Bahru, Malaysia
[2]Department of Electrical and Communication Engineering, College of Engineering, United Arab Emirates University, Al Ain, United Arab Emirates

Article Info

Article history:

Received Jul 9, 2024
Revised Sep 29, 2024
Accepted Oct 7, 2024

Keywords:

Artificial neural network
Machine learning algorithm
Microbial fuel cell
Open circuit voltage
Super vector machine

ABSTRACT

This paper presents the correlation between open circuit voltage (OCV) and pH, temperature, and total dissolved solids (TDS) of an air cathode single chamber microbial fuel cell (MFC) using artificial neural network (ANN) and support vector machine (SVM) algorithms. Previous works used terminal voltages as output parameters to determine the correlation between MFCs' input and output parameters. However, OCV is the most important measurement that can determine the validity of the MFC. Thus, various tests were conducted to analyze the correlation between OCV and input parameters using ANN and SVM algorithms. Both techniques show a strong correlation between OCV and input parameters with the highest R^2 values. The highest OCV value obtained from the experiment is 1.179 V at pH 5.26, temperature 299K, and TDS 3,124 ppm. Furthermore, an ANN model was developed to predict the OCV value based on pH, temperature, and TDS value.

Corresponding Author:

Ganesan V. Murugesu
Department of Electrical Power Engineering, Faculty of Electrical Engineering
Universiti Teknologi Malaysia
Johor Bahru 81310, Malaysia
Email: ganesanvmurugesu@gmail.com

1. INTRODUCTION

Microbial fuel cell (MFC) is an emerging technology that can overtake electricity generation in the future. Even though research into MFC has drastically increased in the past twenty years, the commercialization of MFC still needs to catch up. MFC uses microbes in wastewater to break down pollutants and produce electrons to generate electricity and clean water. An electrode is placed in wastewater, which attracts the electrons to become more negative and is called anode. When the anode is connected to another electrode, called a cathode, through a load, the transfer of electrons from the anode to the cathode occurs and generates electricity [1], [2].

The low power generation and high-cost materials become a bottleneck for the commercialization of the MFC [3]. Many aspects are involved in MFC research to build an excellent system to overcome these issues. However, analyzing and predicting the output voltage is one of the most significant aspects to consider in the development process. Terminal voltage and OCV are the two types of voltages that can be measured in MFC. While many previous studies have used terminal voltage as an output voltage to investigate the impact of input parameters, it does not accurately represent an MFC cell's actual electromotive force (EMF). OCV is a crucial measurement in any electrical source, including batteries and solar cells, when there is no current flow. Therefore, understanding and measuring OCV is paramount in

MFC research [4]. On top of that, an unstable OCV can indicate that the cell has failed and requires modification or replacement [5]. Thus, measuring OCV in fuel cells is essential because it can help determine whether the cell is valid. However, predicting the OCV from the operating condition is a complex task in MFC. Many parameters influence the OCV prediction in MFC, which can be categorized into static and dynamic parameters. The static parameters, such as electrode type, size, distance, proton exchange membrane (PEM), and chamber design, are pre-defined before the chemical reactions start. However, the dynamic parameters, such as substrate concentration, temperature, and pH, pose a challenge to fix throughout the operation [6]. These parameters constantly change during the chemical process, making the system too complex to predict the OCV. This complexity is a fascinating aspect of the research, highlighting the intricacies of OCV in MFC.

OCV was first measured in MFC by Choid *et al.* [7] to investigate its performance using alkalophilic Bacillus sp. Later, many studies were conducted on different aspects to determine the MFC's performance using OCV. However, most of these studies concentrate on improving the OCV with various structures. Only a few studies were conducted to analyze the correlation between input and output parameters due to a lack of technology. However, recent studies use machine learning algorithms (MLA) to predict voltage, power density, and chemical oxygen demand (COD) based on various input parameters. Power density is mainly used as an output parameter to analyze the effect of input parameters such as membrane thickness, external resistance, feed ratio, pH, and temperature [8], [9]. Terminal voltage has also become an essential parameter in a few studies that analyze the correlation between terminal voltage and wastewater concentration, electrode surface, and bacteria count [10]. Table 1 summarizes input and output parameters used in the recent MFC studies using MLA.

Table 1. Input and output parameters considered in recent studies for analysis and optimization techniques of MFC parameters in recent studies

Input parameter	Output parameter	Machine language use for analysis	Optimization techniques	References
Membrane thickness, external resistance, and anode area	PD	SVR	RSM	[8]
Feed ratio of wastes, pH of anode media, and electrode depth	PD	MRA	RSM	[9]
Time, voltage, and current	PD	RFR, ANN and GPR	-	[11]
Phenol concentration and wastewater concentration	V	ANN	SGG and TSM	[10]
Degree of sulphonation, aeration rate, Pt Load	PD, COD	GBR and RFR	PSO	[12]
Yeast concentration and wastewater concentration	PD and COD	ANN	RSM	[13]
Influent COD, VFA, hydraulic retention time, and anode electrode surface area	PD and COD	ANN	-	[14]
Substrate concentration, fuel feed flow rate, and oxygen concentration	PD	ANN	HHO	[15]
Degree of sulphonation, aeration rate, Pt load	V, PD and COD	ANN	SOO and MOO	[16]
Voltage	COD	SVR	-	[17]

PD: power density | V: terminal voltage | COD: chemical oxygen demand | CE: coulombic efficiency | ANN: artificial neural network | RFR: random forests regression | MRA: multiple regression analysis | GBR: gradient boost regression | GPR: gaussian process regression | SVR: support vector regression | PSO: particle swan optimization | SOO: single-object optimization | MOO: multi-object optimization | HHO: Harris Hawk's optimization | SCG: scaled conjugate gradient | TSM: time series model | RSM: response surface methodology

MFC contains various input parameters that influence the output parameter, making the system more complex. So, a single mathematical model is unsuitable for predicting the output parameter. Thus, recent studies widely use MLAs to predict, analyze, and optimize the MFC output [18]. Machine learning is a computer-based algorithm that uses artificial intelligence to solve complex problems. Machine learning uses previous data to learn a system and predict the future output. ANN is the most used MLA in recent studies to predict the output and improve the performance of MFC. Many studies used the ANN model to predict the power density and COD removal using different input variables such as usage of Pt., degree of sulphonation, rate of aeration, phenol concentration, yeast concentration, and wastewater concentration [10]-[16]. Additionally, other MLAs such as Bayesian algorithm (BA), SVM, GBR, and GPR are also widely used to predict the power density, COD and output voltage using membrane thickness, external resistance, and anode area as a inputs [8], [17], [19].

However, the author believes that a study has yet to be conducted to analyze the correlation between a combination of dynamic parameters such as temperature, substrate concentration, and pH value as an input parameter to predict the OCV using MLAs. ANN, GBR, SVM, RFR, MRA, and decision tree regression

(DTR) were selected by the author to compare and choose the most suitable algorithm to be used for MFC analysis. Noisy data, non-linear modal, non-categorical data, large sample size, and complex relationships influence the MFC data set. After analyzing the advantages and disadvantages of each algorithm, as shown in Table 2, the author selects the best two models, SVM and ANN, to be used in this investigation considering the following criteria: (a) data has noise, (b) non-linear modal, (c) non-categorical data, (d) large sample size, and (e) handle complex relationship.

Table 2. The advantages and disadvantages of recent machine learning algorithm used in MFC research

MLA	Advantages	Disadvantage	Reference
GBR	Can handle complex relationships between variables. Better prediction	It required a large dataset for training. Not suitable for noisy data High computational cost Can cause overfitting	[20]
RFR	Easy to understand. Giving accurate prediction Can easily set the parameter	Not suitable for categorical variables	[21]
ANN	It works well with noise. It can have more than one output. Can used for non-linear model	Time consuming It required a large sample size Algorithm structure is challenging to understand.	[21]
DTR	Easy to understand. Order on training has no effect. Fast forecasting. Low computational cost	Cannot overlap the classes It required statistically independent variables Less accurate Pruning is required to avoid overfitting	[21]
SVM	It can work well with noise Can used for non-linear model Can avoid overfitting	Slow training Optimal parameters and algorithm structure are not easy to understand High computational cost	[21]

From the literature review, no study has been conducted to predict the OCV for MFC using the affecting factors, especially the dynamic parameters. This prediction is critically important to detect any failure in MFC and develop any MFC predictive model using the operating conditions. A continuous OCV prediction based on operating conditions while the system is running will help to monitor the performance of the MFC and avoid any failure. So, this study will investigate the correlation between OCV and selected input parameters such as total dissolved solids (TDS), pH, and Temperature to predict the OCV using suitable MLAs.

2. METHOD

The author will investigate the correlation between substrate pH, temperature, and TDS value against the OCV across the anode and the cathode electrode. The first three variables are set as input parameters, and the latter are set as output parameters. A single-chamber air cathode MFC is used in this investigation.

2.1. Construction of chamber

A plastic food container with dimensions 340 mm×240 mm×140 mm (maximum capacity is 10.0 L) is used as the chamber to hold hydrocarbon substrate or anolyte. Then, a hole 40 mm in diameter is cut at the side of the container. Then, a PVC tank connector (40 mm) is fixed in the hole and tested for no leaking. The threaded part of the PVC tank is faced inside the container.

2.2. Preparation of electrodes

The electrodes for this study are meticulously prepared. Two types of electrodes are meticulously prepared: the anode and the cathode. Both the anode and cathode utilize a high-purity carbon graphene sheet, which has high conductivity and is energy-efficient [22]. The anode electrode comprises two sheets of carbon, each measuring 100 mm×100 mm×2 mm. The same material, measuring 70 mm×35 mm×2 mm, is used as a cathode. The anode and cathode electrodes are connected with a 20 mm-length 22 AWG 600 V tinted stranded silicone copper wire, ensuring a secure and reliable connection.

2.3. Preparation of salt bridge

Proton exchange membrane is the best material to use as a separator between anode and cathode chamber. However, a salt bridge is used in this investigation to reduce the cost. A salt bridge is prepared using kalium chloride (KCL) and agar. Ali *et al.* [23] suggested that 1 M of KCL with 5% agar will produce the highest power output. So, 30 g of KCL is mixed with 350 mL of distilled water, and the total volume is added to 400 mL. Then, 20 g of agar is added to the 1 M KCL, mixed gently, and heated with low flame for 2 minutes. Then, the solution is filled into an L-shaped PVC pipe. The L-shaped PVC pipe is prepared using a 5 cm length of 40 mm PVC pipe glued with a 40 mm Elbow. Finally, the cathode electrode is placed inside the PVC pipe elbow, and the prepared liquid is placed in the fridge for 60 minutes to become solid or gel.

2.4. Preparation of synthetic wastewater

For this investigation, synthetic wastewater is selected as an anolyte, with acetate as the primary hydrocarbon. In previous studies, various combinations of chemicals were used to produce synthetic wastewater [24]-[27]. After considering the different combinations of chemicals used earlier, the author decided to use the combination shown in Table 3. Once all the materials are prepared, the plastic chamber is filled with 6.0 L of synthetic wastewater. Then, the anode electrode is immersed inside the synthetic wastewater, and the OCV between the anode and cathode is measured using a digital multimeter. The experimental setup is shown in Figure 1. Figure 1(a) shows the actual photo of the experimental setup, and Figure 1(b) shows the schematic drawing.

Table 3. Preparation of synthetic wastewater (6 L) for this investigation

Chemical	Mg
Manganese (II) chloride ($MnCl_2$)	120
Magnesium dichloride ($MgCl_2$)	960
Calcium chloride ($CaCl_2$)	36
Iron (III) chloride ($FeCl_3$)	12
Ammonium chloride (NH_4Cl)	1,800
Magnesium sulphate ($MgSO_4$)	300
Monopotassium phosphate (KH_2PO_4)	540
Acetate (CH_3COOH)	6,000
Sodium bicarbonate ($NaHCO_3$)	1,800
Yeast	960
Knorr chicken stock	2,000

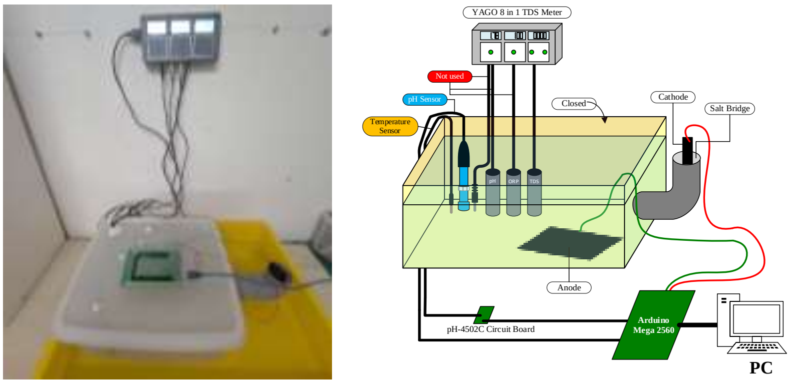

(a) (b)

Figure 1. Experimental setup (a) actual photo and (b) schematic drawing

2.5. Data acquisition procedure

Two different techniques with different meters were used to record the data. An Arduino Mega 2560 R3 microcontroller records the OCV by connecting the cathode to the microcontroller's Analog input. The pH value was recorded using the PH-4502 C sensor, also connected to the microcontroller's analog input. The temperature is recorded using a DS18B20 water-proof temperature sensor connected to the microcontroller's digital input. All the data was recorded every 15 seconds and sent to Microsoft Excel. Then, the recorded data is downloaded manually every 12 hours in a separate worksheet for further use.

On the other hand, TDS were recorded using an 8-in-1 YAGO WIFI smart water detector. The data recorder for every minute from this meter is manually sent to email and then downloaded into Excel format for further analysis. The data is recorded every 15 seconds using an Arduino microcontroller (OCV, temperature, and pH) and continuously every minute using a TDS sensor (TDS) for ten days. However, for the analysis purpose, only twelve sets of data are taken in an hour with an interval of 5 minutes per data. Thus, 2,880 sets of data (12 per hour×24 hours×10 days=2,880) were analyzed.

2.6. Data selection

The correlation between the input and output parameters is determined by plotting fitting curves using MATLAB software. Figure 2 shows the OCV changes in the first ten days. The MFC is fed with wastewater whenever voltage drops are noted. The data shows that the OCV increases when wastewater is added. The relationship between the OCV and the input parameters is initially developed using the min-max scaling normalization method using (1). Then, the three graphs are plotted to view the relationship between input and output parameters in Figure 3; Figure 3(a) the relationship between pH and OCV, Figure 3(b) shows the relationship between temperature and OCV and Figure 3(c) shows the relationship between TDS and OCV.

$$x_{norm} = \frac{x - x_{min}}{x_{max} - x_{min}} \times 100 \quad (1)$$

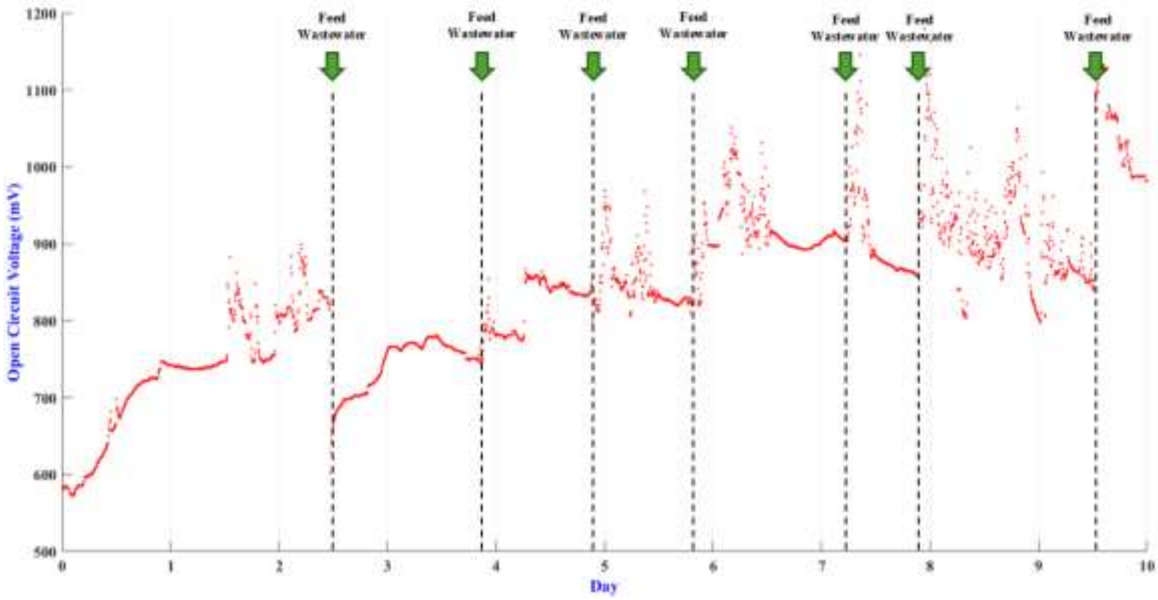

Figure 2. The OCV was measured in ten days

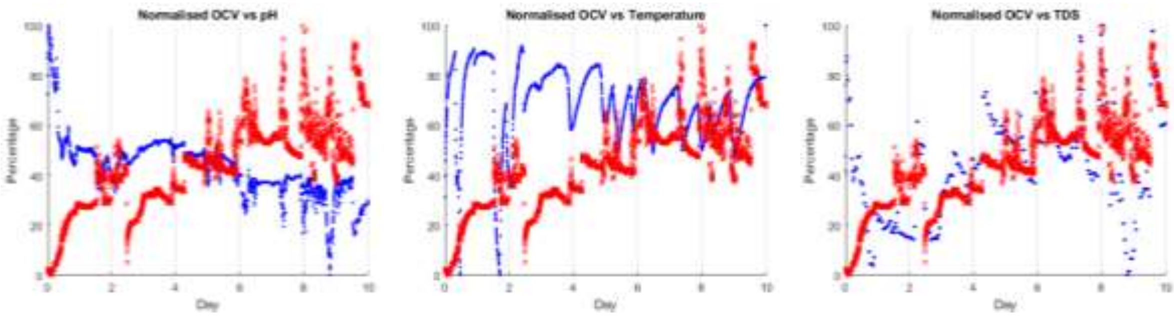

(a) (b) (c)

Figure 3. The relationship between normalized OCV (Red,'x') and the other three inputs (Blue, '.') (a) pH, (b) temperature, and (c) TDS for 10 days

The plot shows that the relationship between input and output is inconsistent for the first 2½ days. However, after that, there is a good relationship between input and output, which shows that temperature and TDS are proportional to the OCV, and pH is inversely proportional to the OCV. So, the author concluded that the MFC takes an initial delay to become stable enough to react to the surrounding condition. Thus, the first 720 sets of data (2.5 days) are removed, which is considered a buffer zone for the MFC to get into a stable condition. The total data sets become 7.5 days×12×24=2,160. From these data, 60% is allocated for training, 20% for validation, and 20% for testing, as shown in Table 4. Figure 4 shows the new plot showing the relationship between input and output parameters for 7½ days; Figure 4(a) shows the relationship between pH and OCV, Figure 4(b) shows the relationship between temperature and OCV, and Figure 4(c) shows the relationship between TDS and OCV.

Table 4. The number of samples for training, validation, and test set

Date type	Percentage	Total sets of data	Sample no.
Training	60%	1,296	1 to 1,296
Validation	20%	432	1,297 to 1,728
Testing	20%	432	1,729 to 2,160

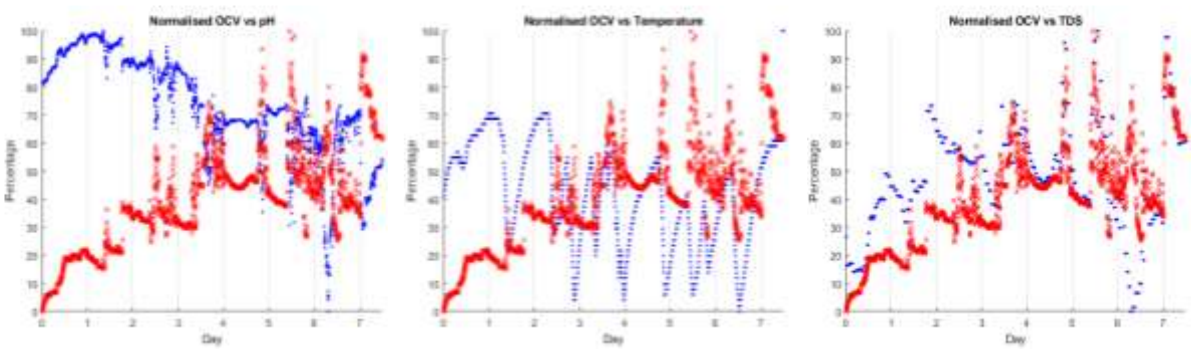

(a) (b) (c)

Figure 4. The relationship between normalized OCV (Red) and the other three inputs (Blue) (a) pH, (b) temperature, and (c) TDS for 7½ Days

3. RESULTS AND DISCUSSION

This section presents the result obtained from the MLA using ANN and SVM models. Then, the testing and validating results are discussed. Finally, the neural network fitting is proposed for future works.

3.1. Predict the OCV using ANN algorithm

ANN was applied to determine the correlation between pH, temperature, and TDS against the OCV. The network has three input and one output neuron . The number of hidden layers was set to one to three, and the number of nodes was set to 10, 25, and 100 to decide the best architecture. The result is shown in Table 5. From Table 5, the author selects model ANN8 as a suitable model for further prediction, considering that this model gives the highest R-squared value (0.9898), low RMSE values, and low training time. Even though model ANN9 gives the lowest RMSE value, the training time and model size are slightly higher for this model. Figure 5 shows the output result for training data using a tri-layered ANN model with 25 fully connected layers. Figure 5(a) shows the OCV-record number relationship, Figure 5(b) shows the OCV-pH relationship, Figure 5(c) shows the OCV-temperature relationship, and Figure 5(d) shows the OCV-TDS relationship for actual and predicted result. Figure 5(e) shows the relationship between measured and predicted OCV.

Table 5. Comparison between different settings of the ANN model

Model ref. number	Number of layers	Number of nodes	RMSE	R-squared value	MSE	MAE	Training time (s)	Model size (kB)
ANN1	1	10	16.763	0.9506	311.90	12.224	5.8787	5
ANN2	1	25	15.535	0.9576	168.36	9.086	7.1927	6
ANN3	1	100	15.169	0.9596	142.88	7.828	10.575	9
ANN4	2	10	12.904	0.9708	185.95	8.943	5.8559	7
ANN5	2	25	14.614	0.9625	148.02	7.856	9.5445	12
ANN6	2	100	7.0736	0.9912	47.597	4.354	19.559	88
ANN7	3	10	9.8942	0.9828	122.19	6.933	8.2325	9
ANN8	3	25	7.6525	0.9898	61.61	5.086	11.103	18
ANN9	3	100	5.3743	0.9949	31.46	3.416	29.527	168

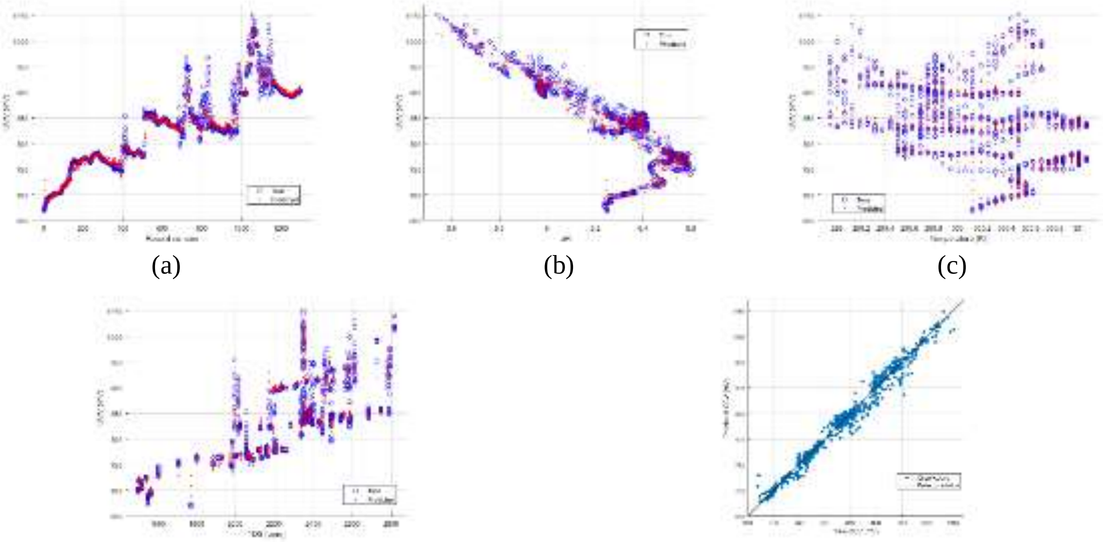

(a) (b) (c)

(d) (e)

Figure 5. The output result of the predicted OCV (Red '.') vs True Value (Blue 'o') using model ANN8: (a) OCV vs. record numbers, (b) OCV vs. pH, (c) OCV vs. temperature, (d) OCV vs. TDS, and (e) actual vs predicted OCV

3.2. Predict the OCV using the SVM algorithm

The training data was also tested using the SVM algorithm. Six different properties are used to train the data, and the best algorithm is selected based on the lowest R-squared value and fastest training time. The result of six different types of SVM algorithms is shown in Table 6. According to the analysis, model 5, medium gaussian SVM (SVM5), is the best model for further study, giving a 0.98 R-squared value, 93.89 MSE, and 1.0107s training time. Figure 6 shows the output result of the predicted OCV and actual value against various parameters using the SVM algorithm. Figure 6(a) shows the OCV-record number relationship, Figure 6(b) shows the OCV-pH relationship, Figure 6(c) shows the OCV-temperature relationship and Figure 6(d) shows the OCV-TDS relationship for actual and predicted results. Figure 6(e) shows the relationship between measured and predicted OCV. Both models show that the TDS value significantly predicts the output with a 1.9656 score and the other two parameter temperature and pH scores of 1.5181 and 1.0757, respectively, as shown in Figure 7.

Table 6. Comparison between different models of SVM algorithms

Model ref. number	Model name	RMSE	R-squared value	MSE	MAE	Training time (s)	Model size (kB)
SVM1	Linear SVM	20.241	0.93	409.71	12.280	5.20	18
SVM2	Quadratic SVM	15.440	0.96	238.39	9.774	3.70	17
SVM3	Cubic SVM	12.077	0.97	145.86	7.727	38.6	14
SVM4	Fine gaussian SVM	10.991	0.98	120.80	6.924	2.74	10
SVM5	Medium gaussian SVM	9.815	0.98	96.33	6.383	1.98	11
SVM6	Coarse gaussian SVM	15.139	0.96	229.20	0.960	4.55	16

3.3. Testing and validating the data using ANN and SVM algorithms

From sections 3.1 and 3.2, the author selects a tri-layered ANN with 25 fully connected layers (ANN8) and a medium gaussian SVM (SVM5) algorithm to train the data. The same models are used to test and validate 864, or 40% of the collected data. The output result is shown in Table 7, and the predicted and actual OCV is illustrated in Figures 8 and 9. Both testing and validating data using ANN and SVM models show that the data is perfectly suitable for further application with the highest R-square value. Figure 8(a) shows the relationship between OCV and record number, and Figure 8(b) shows the relationship between actual and predicted OCV for validation data using the ANN algorithm. Figure 8(c) shows the relationship between OCV and record number, and Figure 8(d) shows the relationship between actual and predicted OCV for validation data using the SVM algorithm.

Figure 9(a) shows the relationship between OCV and record number, and Figure 9(b) shows the relationship between actual and predicted OCV for testing data using the ANN algorithm. Figure 9(c) shows the relationship between OCV and record number, and Figure 9(d) shows the relationship between actual and predicted OCV for testing data using the SVM algorithm.

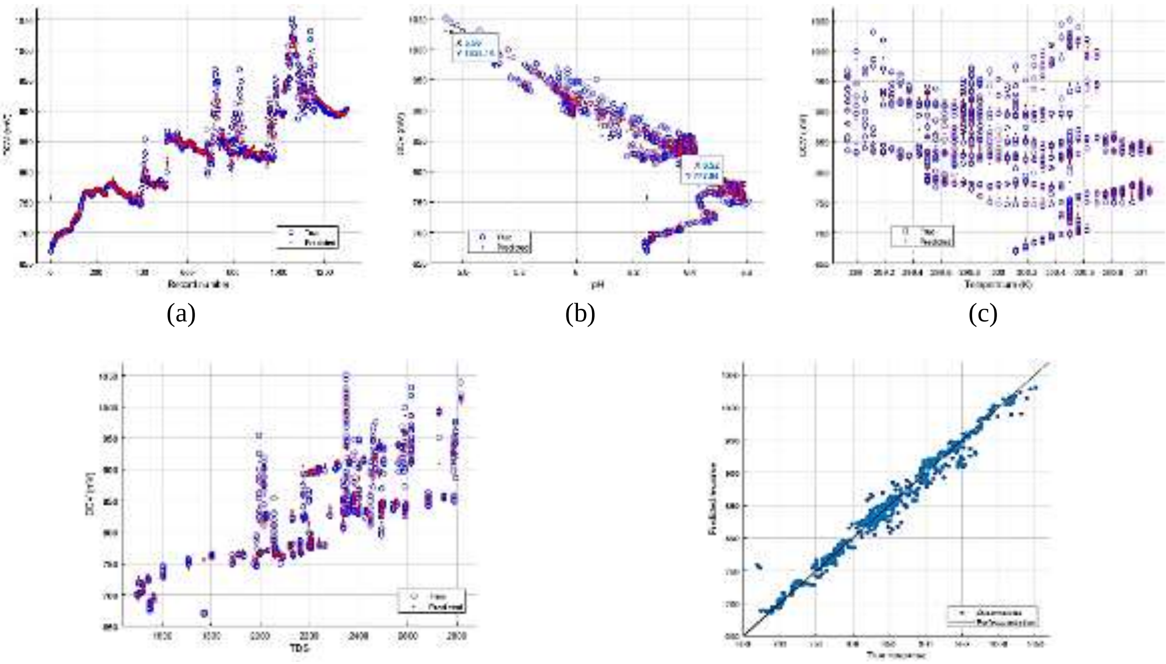

Figure 6. The output result of the predicted OCV (Red, '.') vs true value (Blue, 'o') using model SVM5: (a) OCV vs. record numbers, (b) OCV vs. pH, (c) OCV vs. temperature, (d) OCV vs. TDS, and (e) actual vs predicted OCV

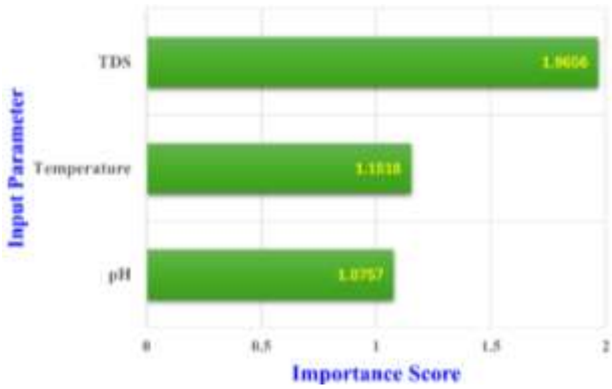

Figure 7. The importance score sorted using mean-redundancy-maximum-relevance (MRMR) algorithm

Table 7. The output result for testing and validation data using ANN and SVM

Model Ref. number	Model name	RMSE	r-squared value	MSE	MAE	Training time (s)	Model size (kB)
Data validation	Tri-layered ANN (ANN8)	7.7986	0.9855	60.819	4.7125	2.75	18
	Medium gaussian SVM (SVM5)	10.393	0.9741	108.02	5.6921	0.57	9
Data testing	Tri-layered ANN (ANN8)	6.2417	0.9900	38.959	3.7343	2.13	18
	Medium gaussian SVM (SVM5)	9.1239	0.9900	83.246	7.0638	0.55	7

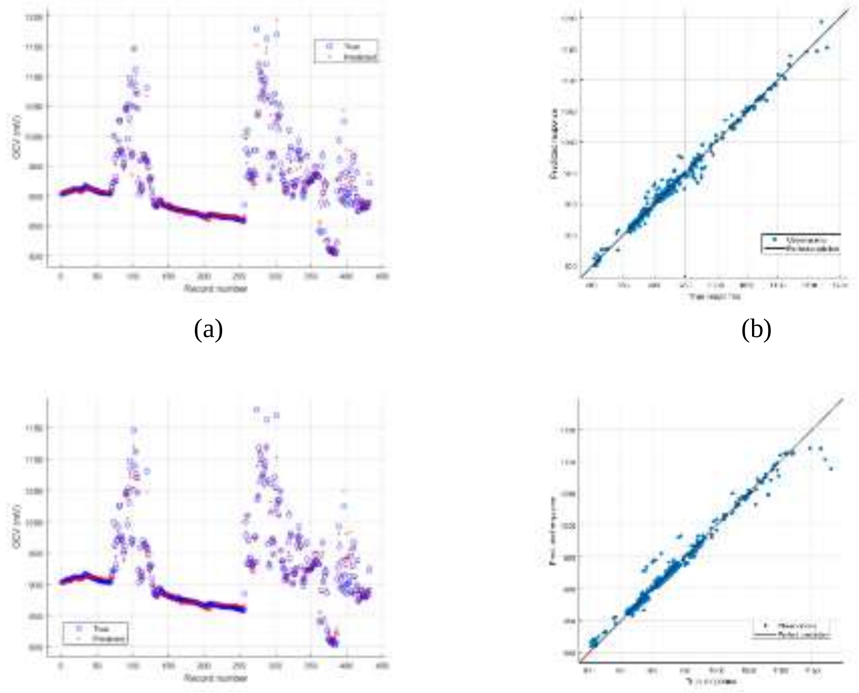

(a) (b)

(c) (d)

Figure 8. The validation result: (a) OCV vs. record numbers using ANN, (b) predicted vs. true response using ANN, (c) OCV vs. record numbers using SVM, and (d) predicted vs. true response using SVM

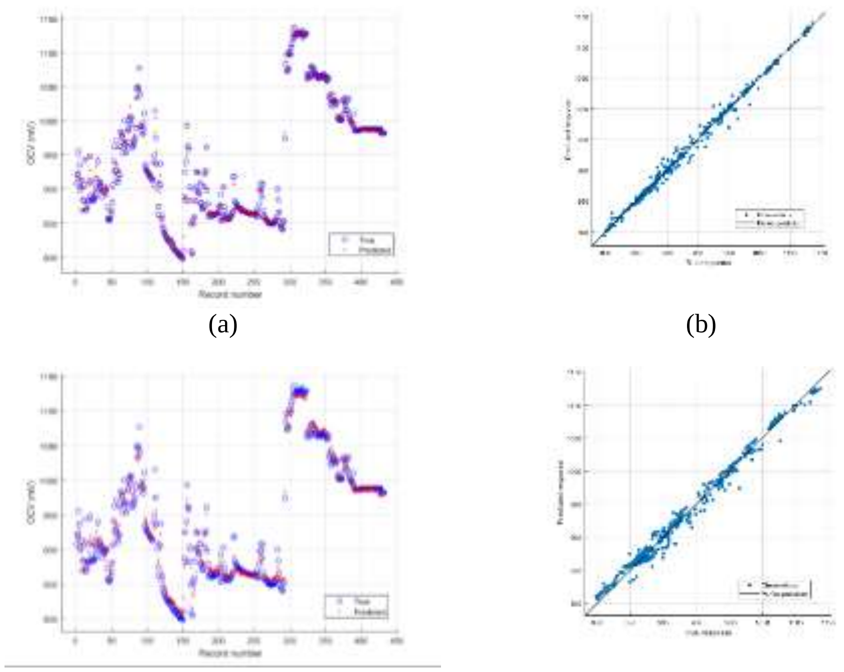

(a) (b)

(c) (d)

Figure 9. The test result: (a) OCV vs. record numbers using ANN, (b) predicted vs. true response using ANN, (c) OCV vs. record numbers using SVM, (d) predicted vs. true response using SVM

3.4. Neural net fitting

Neural net fitting is simulated with 25 layers, as suggested in section 3.1. This is the most appropriate setting to compile an extensive data set with minimum time, the highest R^2 value, and the lowest

MSE. The system becomes more complex when the number of hidden layers is increased, so a powerful supercomputer is required to compile the data. Figure 10 shows the output result for the collected data.

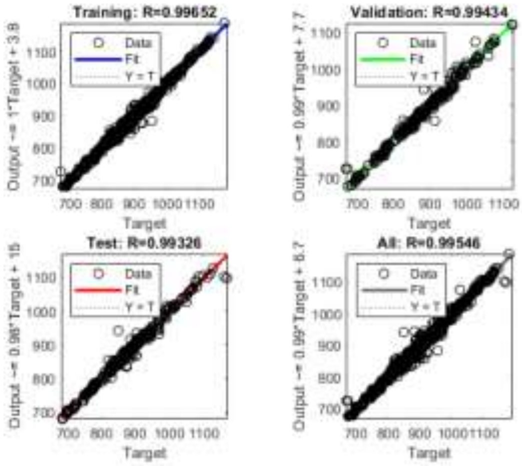

Figure 10. Neural net fitting output using 25 hidden layers

Using the ANN model, the author simulates the output value for a selected 30 data sets by fixing one of the input parameters as a constant to show the difference between measured and predicted output, as shown in Figure 11. In sample Figure 11(a), the temperature is fixed at 300K; in sample Figure 11(b), the pH value is fixed between 5.40 and 5.50; and in sample Figure 11(c), the TDS value is fixed between 2,300 and 2,350. The result shows that the error between the measured and the predicted value is less than 10 mV.

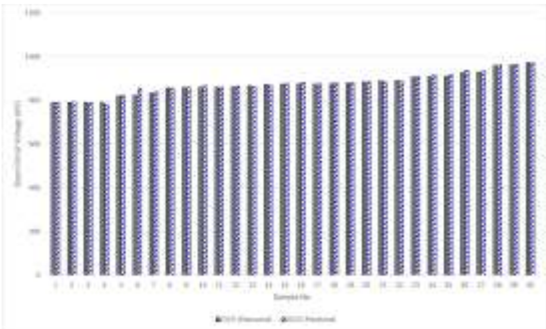

(a)

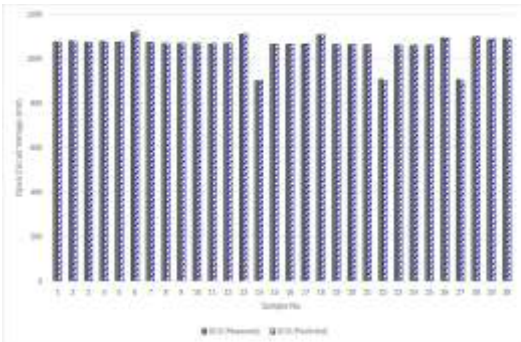

(b)

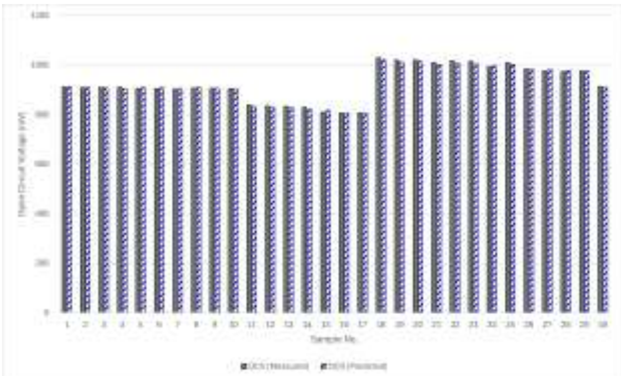

(c)

Figure 11. The comparison between measured and predicted OCV (mV) at: (a) constant temperature, (b) constant pH, and (c) constant concentration

4. CONCLUSION

The highest OCV generated from this research work is 1.179 V at pH 5.26, Temperature 299K, and TDS 3,124 ppm. These three parameters substantially impact determining the MFC's OCV. The ANN and SVM algorithms show a strong correlation between input and output parameters with 0.99 and 0.98 correlation coefficients (R^2), respectively. A comparison between the ANN and SVM models gives almost compatible results, showing that both are suitable for MFC design. The neural net fitting model, which shows the lowest error between the predicted and actual OCV, is ideal for the MFC as an OCV predictor.

The analysis shows a strong correlation between MFC's OCV and the input parameters TDS, pH, and temperature. However, the TDS value dominates the OCV's prediction. So, changing the TDS value by adding wastewater or distilled water to substrates can adjust the OCV in MFC. This result is useful for future designs that balance the voltages by adjusting the TDS between MFCs connected in series or parallel.

While this research's conclusion is informative, some limitations remain, which can be upgraded. Future studies should examine the model with variable loads. Additionally, employing actual wastewater as a substrate may enhance the model further. This work is considered a booster for the ongoing research in this field to generate a voltage-balanced MFC model in series or parallel.

ACKNOWLEDGEMENTS

The author thanks the Ministry of Higher Education for supporting/funding this work under the Fundamental Research Grant Scheme (FRGS/1/2023/TK07/UTM/02/36).

REFERENCES

[1] A. Salvian *et al.*, "Resilience of anodic biofilm in microbial fuel cell biosensor for BOD monitoring of urban wastewater," *npj Clean Water,* vol. 7, no. 1, 2024, doi: 10.1038/s41545-024-00350-5.

[2] D. K. Zater, F. I. Elzamik, H. M. Abdel Basit, G. E. D. M. Moustafa, D. Z. Khater, and K. M. El-Khatib, "Investigating the bacterial consortia properties of electrogenic anodic biofilm in a double-chamber microbial fuel cell: electrochemical, physical, biochemical and molecular characterization," *Sustainable Environment Research,* Article vol. 34, no. 1, 2024, Art no. 9, doi: 10.1186/s42834-024-00215-z.

[3] J. Wang, K. Ren, Y. Zhu, J. Huang, and S. Liu, "A review of recent advances in microbial fuel cells: preparation, operation, and application," *BioTech,* Review vol. 11, no. 4, 2022, Art no. 44, doi: 10.3390/biotech11040044.

[4] M. Rahimnejad, "Chapter 5 - Energy and power measurement methods in MFCs," in *Biological Fuel Cells*, M. Rahimnejad Ed.: Elsevier, 2023, pp. 127-146.

[5] J. Zhang, H. Zhang, J. Wu, and J. Zhang, "Chapter 7 - Fuel cell open circuit voltage," in *Pem Fuel Cell Testing and Diagnosis*, Eds. Amsterdam: Elsevier, 2013, pp. 187-200.

[6] G. V. Murugesu, S. N. Khalid, and H. Shareef, "Microbial fuel cell as a future energy source: a review of its development, design, power generation, and voltage reversal control mechanism," *IEEE Access,* vol. 10, pp. 128022-128045, 2022, doi: 10.1109/ACCESS.2022.3227433.

[7] A. Choid, A. Youngjin, J. Song, S. Jung, and S. Kim, "Optimization of the performance of microbial fuel cells containing alkalophilic Bacillus sp," *Journal of Microbiology and Biotechnology,* Article vol. 11, no. 5, pp. 863-869, 2001.

[8] S. M. Z. Hossain, N. Sultana, S. Haji, S. T. Mufeez, S. E. Janahi, and N. A. Ahmed, "Modeling of microbial fuel cell power generation using machine learning-based super learner algorithms," *Fuel,* Article vol. 349, 2023, Art no. 128646, doi: 10.1016/j.fuel.2023.128646.

[9] S. Mandal *et al.*, "Generation of bio-energy after optimization and controlling fluctuations using various sludge activated microbial fuel cell," *Environmental Science and Pollution Research,* Article 2023, doi: 10.1007/s11356-023-26344-3.

[10] M. Ghasemi, A. M. Nassef, M. Al-Dhaifallah, and H. Rezk, "Performance improvement of microbial fuel cell through artificial intelligence," *International Journal of Energy Research,* Article vol. 45, no. 1, pp. 342-354, 2021, doi: 10.1002/er.5484.

[11] K. Singh, "Power density analysis by using soft computing techniques for microbial fuel cell," *Journal of Environmental Treatment Techniques,* Article vol. 7, no. Special Issue, pp. 1068-1073, 2019.

[12] Y. Abdollahfard, M. Sedighi, and M. Ghasemi, "A new approach for improving microbial fuel cell performance using artificial intelligence," *Sustainability (Switzerland),* Article vol. 15, no. 2, 2023, Art no. 1312, doi: 10.3390/su15021312.

[13] E. T. Sayed, H. Rezk, M. A. Abdelkareem, and A. G. Olabi, "Artificial neural network based modelling and optimization of microalgae microbial fuel cell," *International Journal of Hydrogen Energy,* Article 2023, doi: 10.1016/j.ijhydene.2022.12.081.

[14] R. Gurjar and M. Behera, "Integrating operating conditions to develop a neural network for predicting organics removal and power density in an earthen microbial fuel cell treating leachate," *Biofuels,* Article vol. 14, no. 1, pp. 49-58, 2023, doi: 10.1080/17597269.2022.2116769.

[15] H. Rezk, A. G. Olabi, M. A. Abdelkareem, and E. T. Sayed, "Boosting the power density of two-chamber microbial fuel cell: Modeling and optimization," *International Journal of Energy Research,* Article vol. 46, no. 15, pp. 20975-20984, 2022, doi: 10.1002/er.8589.

[16] S. Naik and J. S. Eswari, "Experimental and validation with neural network time series model of microbial fuel cell bio-sensor for phenol detection," *Journal of Environmental Management,* Article vol. 290, 2021, Art no. 112594, doi: 10.1016/j.jenvman.2021.112594.

[17] F. Shabani, H. Philamore, and F. Matsuno, "An energy-autonomous chemical oxygen demand sensor using a microbial fuel cell and embedded machine learning," *IEEE Access,* Article vol. 9, pp. 108689-108701, 2021, Art no. 9502709, doi: 10.1109/ACCESS.2021.3101496.

[18] J. Huang, Y. Gao, Y. Chang, J. Peng, Y. Yu, and B. Wang, "Machine learning in bioelectrocatalysis," *Advanced Science,* Review vol. 11, no. 2, 2024, Art no. 2306583, doi: 10.1002/advs.202306583.

[19] M. O. Oyedeji, A. Alharbi, M. Aldhaifallah, and H. Rezk, "Optimal data-driven modelling of a microbial fuel cell," *Energies*, Article vol. 16, no. 12, 2023, Art no. 4740, doi: 10.3390/en16124740.
[20] A. Natekin and A. Knoll, "Gradient boosting machines, a tutorial," *Frontiers in Neurorobotics*, Article vol. 7, no. DEC, 2013, Art no. Article 21, doi: 10.3389/fnbot.2013.00021.
[21] J. Charoenpong, B. Pimpunchat, S. Amornsamankul, W. Triampo, and N. Nuttavut, "A comparison of machine learning algorithms and their applications," *International Journal of Simulation--Systems, Science and Technology*, vol. 20, no. 4, 2019.
[22] A. Starowicz, M. Zieliński, P. Rusanowska, and M. Dębowski, "Microbial fuel cell performance boost through the use of graphene and its modifications—review," *Energies*, Review vol. 16, no. 2, 2023, Art no. 576, doi: 10.3390/en16020576.
[23] A. Ali, H. Al-Mussawy, M. Hussein, and N. Hamadi, "Experimental and theoretical study on the ability of microbial fuel cell for electricity generation," *Pollution*, vol. 4, no. 2, pp. 359-368, 2018.
[24] S. Gadkari, J.-M. Fontmorin, E. Yu, and J. Sadhukhan, "Influence of temperature and other system parameters on microbial fuel cell performance: Numerical and experimental investigation," *Chemical Engineering Journal*, vol. 388, p. 124176, 2020, doi: 10.1016/j.cej.2020.124176.
[25] I. Apostolopoulos *et al.*, "The effect of anode material on the performance of a hydrogen producing microbial electrolysis cell, operating with synthetic and real wastewaters," *Energies*, Article vol. 14, no. 24, 2021, Art no. 8375, doi: 10.3390/en14248375.
[26] L. Cristiani, M. Zeppilli, G. Fazi, C. Marandola, and M. Villano, "Renewable gases production coupled to synthetic wastewater treatment through a microbial electrolysis cell," *Biochemical Engineering Journal*, Article vol. 205, 2024, Art no. 109249, doi: 10.1016/j.bej.2024.109249.
[27] Z. Ullah and S. Zeshan, "Effect of substrate type and concentration on the performance of a double chamber microbial fuel cell," *Water Science and Technology*, vol. 81, no. 7, pp. 1336-1344, 2020, doi: 10.2166/wst.2019.387.

BIOGRAPHIES OF AUTHORS

Ganesan V. Murugesu received his B.Eng. Degree in Electrical and Electronic Engineering from Universiti Sains Malaysia, Perak, Malaysia, in 1999 and his Master's degree in Electrical and Electronic Engineering from Universiti Teknologi Malaysia, Johor, Malaysia, in 2009. He is currently pursuing a Ph.D. degree in the same field at Universiti Teknologi Malaysia, Johor, Malaysia. He can be contacted at email: ganesanvmurugesu@gmail.com.

Saiful Nizam Khalid received his B.Eng. degree (1998), M.E.E. (2000), and Ph.D. (2009) from Universiti Teknologi Malaysia. His research interests include deregulated power systems, the application of artificial neural networks in power systems, power tracing, and smart metering applications. He is an associate professor of Electrical Engineering at Universiti Teknologi Malaysia, Johor Bahru, Malaysia. He can be contacted at email: saifulnizam@utm.my.

Prof. Dr. Hussain Shareef (Member, IEEE) received a Ph.D. in Electrical Engineering from Universiti Teknologi Malaysia (UTM), Malaysia, in 2007. He is currently a Professor at the Department of Electrical Engineering at United Arab Emirates University. He is the Head of the Green Mobility Research Team at the Emirates Center for Mobility Research. Since the Ph.D. degree, he has published more than 400 peer-reviewed journal articles in various fields related to power and energy systems. He has more than 10,000 citations with an H-index of 52. His research interests include power system planning, integration of renewable power sources, application of AI techniques in power systems, energy management, power quality, and electric vehicle grid integration. He is a member of the Mohammed Bin Rashid Academy of Scientists. Among his many awards, he was a 2019–2020 recipient of the UAE University Award for Excellence in Scholarship and the Chancellor Innovation Award (2020–2021). Stanford University listed him as the World's Top 2% Scientist from 2019 to 2023. He can be contacted at email: shareef@uaeu.ac.ae.

Saad Saleem Khan received his B.S. and M.S. degrees in Electrical Engineering Power from the University of Engineering and Technology Lahore, Pakistan. He completed his Ph.D. at Arab Emirates University, UAE. He is currently a part-time post-doc researcher at the United Arab Emirates University and also Deputy Manager of Technical at National Transmission and Despatch Company Limited, Pakistan. He is currently doing research on applications, modeling, and fault diagnosis of fuel cells. He can be contacted at email: saadkhanopf@gmail.com.